HHS Public Access

Author manuscript

Acta Biomater. Author manuscript; available in PMC 2020 July 15.

Published in final edited form as:

Acta Biomater. 2019 July 15; 93: 210–221. doi:10.1016/j.actbio.2019.01.045.

Decorin-Supplemented Collagen Hydrogels for the Co-Delivery of Bone Morphogenetic Protein-2 and Microvascular Fragments to a Composite Bone-Muscle Injury Model with Impaired Vascularization☆

Marissa A. Ruehle[a,b], **Mon-Tzu Alice Li**[a,b], **Albert Cheng**[a,c], **Laxminarayanan Krishnan**[a], **Nick J. Willett**[a,b,d,e], **Robert E. Guldberg**[a,f]

[a]Parker H. Petit Institute for Bioengineering and Bioscience, Georgia Institute of Technology, Atlanta, GA, USA

[b]Wallace H. Coulter Department of Biomedical Engineering, Georgia Institute of Technology & Emory University, Atlanta, GA, USA

[c]George W. Woodruff School of Mechanical Engineering, Georgia Institute of Technology, Atlanta, GA, USA

[d]Department of Orthopedics, Emory University, Atlanta, GA, USA

[e]Atlanta Veteran's Affairs Medical Center, Decatur, GA, USA

[f]Knight Campus for Accelerating Scientific Impact, University of Oregon, Eugene, OR, USA

Abstract

Traumatic musculoskeletal injuries that result in bone defects or fractures often affect both bone and the surrounding soft tissue. Clinically, these types of multi-tissue injuries have increased rates of complications and long-term disability. Vascular integrity is a key clinical indicator of injury severity, and revascularization of the injury site is a critical early step of the bone healing process. Our lab has previously established a pre-clinical model of composite bonemuscle injury that exhibits impaired bone healing; however, the vascularization response in this model had not yet been investigated. Here, the early revascularization of a bone defect following composite injury is shown to be impaired, and subsequently the therapeutic potential of combined vascularization and osteoinduction was investigated to overcome the impaired regeneration in composite injuries. A decorin (DCN)-supplemented collagen hydrogel was developed as a biomaterial delivery vehicle for the co-delivery microvascular fragments (MVF), which are multicellular segments of mature vasculature, and bone morphogenetic protein-2 (BMP-2), a potent osteoinductive growth factor.

☆Part of the Drug Delivery for Musculoskeletal Applications Special Issue, edited by Robert S. Hastings and Professor Johnna S. Temenoff.

Address correspondence to: Robert E. Guldberg, Knight Campus for Accelerating Scientific Impact, 6231 University of Oregon, Eugene, OR 97403-6231; Phone 541-346-3110, guldberg@uoregon.edu.

We hypothesized that collagen+DCN would increase BMP-2 retention over collagen alone due to DCN's ability to sequester TGF-ß growth factors. We further hypothesized that MVF would increase both early vascularization and subsequent BMP-2-mediated bone regeneration. Contrary to our hypothesis, BMP+MVF decreased the number of blood vessels relative to BMP alone and had no effect on bone healing. However, collagen+DCN was demonstrated to be a BMP-2 delivery vehicle capable of achieving bridging in the challenging composite defect model that is comparable to that achieved with a well-established alginate-based delivery system.

Graphical Abstract:

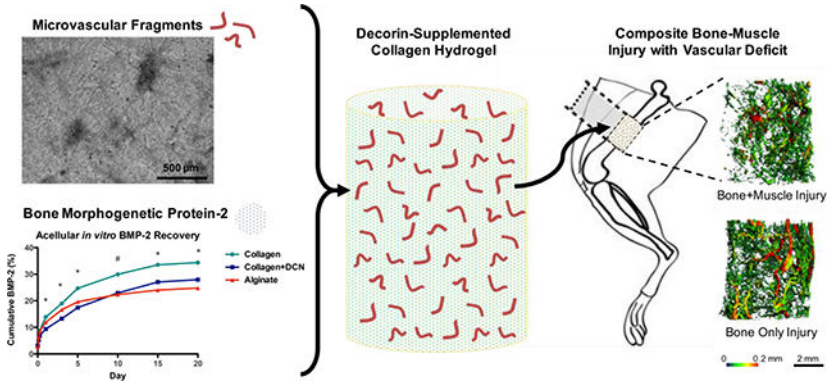

Keywords

composite musculoskeletal injury; vascularization; collagen decorin hydrogel; microvascular fragments; bone morphogenetic protein

1. INTRODUCTION

Traumatic musculoskeletal injuries resulting in open fractures, which are characterized by concomitant soft tissue injury, represent a major clinical challenge. Cases of open fracture have a two-fold increased rate of complications including infection, delayed union, malunion, and nonunion compared to closed fractures [1]. These complications often lead to repeated surgical interventions that are still not able to avert long-term disability 7 years following injury [2]. One of the key clinical indicators of composite injury severity is vascular integrity; composite injuries that include vascular damage are considered the most severe [3]. We have previously established a pre-clinical rat model of composite bone-muscle extremity injury that recapitulates the attenuation of bone healing seen clinically [4], and similar pre-clinical models have also observed impaired bone healing with concomitant muscle injury [5, 6]. However, the vascularization response following injury has not been previously investigated in the composite defect model.

Early revascularization is a critical step of the wound healing cascade, providing a transport mechanism for oxygen, pro-regenerative growth factors, and stem and progenitor cells [7]. When vascularization is impaired in fracture models, bone healing is also severely impaired [8, 9]. Osteoprogenitor cells migrate into the bone defect region along with nascent vasculature, and osteoprogenitor cells and endothelial cells participate in bidirectional

chemical signaling to stimulate growth [10]. As such, vascularization has been a promising target in bone regeneration, and many previous strategies have been employed including the co-delivery of osteogenic and angiogenic growth factors (e.g. bone morphogenetic protein-2 (BMP-2) vascular endothelial growth factor (VEGF)) as well as mesenchymal stem cell (MSC) and endothelial cell delivery [11]. However, while some growth factor co-delivery strategies report an improvement in healing [12–14], others report only a temporary transient effect or no effect at all [15–18]. Although endothelial cell-based strategies have been shown to increase bone regeneration [19, 20], the resultant vasculature is often immature and leaky [21]. Another promising option is the use of microvascular fragments (MVF), which are multicellular segments of mature vasculature [22]. MVF are able to serve as a template for vascular growth and thus accelerate the establishment of vascular networks. Additionally, MVF retain vascular support cells and may therefore accelerate vessel maturation and patency. MVF form networks in vitro and have been previously shown to anastomose with host vasculature [23, 24] and increase tissue vascular volume [25] following implantation. Previous vascularization therapies without an osteoinductive factor have not improved bone healing [18, 26]. Therefore, we investigated the co-delivery of MVF with BMP-2, a potent osteoinductive growth factor.

Design criteria for a co-delivery biomaterial are the support of MVF growth and sustained BMP-2 release. MVF have typically been cultured in type I collagen gels, which support in vitro sprouting and network formation [22, 25]. However, collagen-based materials tend to have a burst release of BMP-2 [27], which necessitates supraphysiological dosing and can cause exuberant bone formation outside the defect site [28]. Biomaterials with a more sustained BMP-2 release profile, such as alginate, have shown improved healing compared to collagen sponge [29]. MVF are sensitive to their extracellular matrix [30, 31], and we have previously developed a decorin-supplemented collagen culture substrate that supports robust angiogenesis of MVF [32]. Decorin (DCN) is a small leucine-rich proteoglycan naturally found in connective tissue [33]. DCN alters collagen fibrillogenesis, which in turn affects the mechanical properties of collagen hydrogels [32, 34] and limits the cell-mediated contraction of collagen [32].This increased dimensional stability allows vessel networks to grow and exert traction forces without collapsing the collagen matrix. DCN has also been shown to sequester transforming growth factor ß (TGF-ß) family growth factors [35, 36], such as BMP-2, which may allow for a more sustained release as compared to collagen alone.

Here, we first investigated the early revascularization response of an established model of composite bone-muscle injury. Since the model recapitulates the impaired bone healing observed clinically, we hypothesized that early vascularization, a key clinical indicator of composite injury healing, would be decreased compared to bone injury alone. Based on our results, we then evaluated decorin-supplemented collagen hydrogels (collagen+DCN) as a biomaterial vehicle for the co-delivery of BMP-2 and MVF. We hypothesized that collagen +DCN would increase BMP-2 retention over collagen alone due to DCN’s ability to sequester TGF-ß growth factors. We further hypothesized that MVF would increase both early vascularization and subsequent BMP-2-mediated bone regeneration.

2. METHODS

All animal experiments were performed in accordance with protocols approved by the Georgia Institute of Technology Institutional Animal Care and Use Committee (IACUC).

2.1 Early Revascularization Following Composite Injury

2.1.1 Surgical Procedures—Unilateral segmental bone defects were made in 13-week-old female Sprague-Dawley rats by creating a critical size 8 mm femoral defect stabilized by internal fixation (bone only defect group) [37]. Composite defects were made by creating an overlying 8 mm diameter full-thickness quadriceps femoris muscle defect in addition to the segmental bone defect as previously described (composite defect group) [4]. All bone defects received 2 μg BMP-2 (Pfizer, Inc.; New York, NY) delivered in RGD-alginate gel injected into an electrospun polycaprolactone (PCL) nanofiber mesh tube approximately 300–400 μm thick with 1 mm perforations as previously described [38]. 23 animals were used to compare revascularization at early time points; animals were euthanized at days 3 (n=7/group), 7 (n=7), and 14 (n=9) post-surgery to assess vascularization using micro-computed tomography (μCT) angiography.

2.1.2 μCT Angiography—Animals were sequentially perfused with 0.9% saline to clear blood vessels, 0.4% papaverine hydrochloride to dilate vessels, 10% neutral buffered formalin to fix, saline to rinse, and a lead chromate radiopaque contrast agent (Microfil MV-22 diluted 2:1; Flow Tech, Inc., Carver, MA). Samples were stored overnight at 4 °C to allow complete polymerization of the contrast agent prior to dissection and μCT analysis. Hind limbs from the hip to the knee were excised. For day 3 and day 7 samples, no bone had yet formed in the defect area and limbs were analyzed immediately. For day 14 samples, the samples were immersed in decalcification solution (Cal-Ex II, Fisher Scientific; Hampton, NH) for a period of 2–3 weeks under gentle agitation with solution changes every 1–3 days prior to analysis.

Two volumes of interest (VOIs) were used to analyze either the bone defect region only or the entire thigh, including both the bone defect and surrounding muscle. For the early revascularization study, scans were performed at a 38 μm voxel size for vessels within the thigh and a 21 μm voxel size for vessels within the bone defect. The thigh VOI encompassed the entire diameter of the thigh for the length of the defect, and the bone defect VOI consisted of a cylindrical volume 6 mm in diameter to encompass the outer diameter of the treatment-containing PCL mesh tube. A global threshold was applied for segmentation of vasculature, and a Gaussian low-pass filter was used to suppress noise ($\sigma = 0.8$, support = 1). Total vascular volume and voxel diameter histograms were computed using native Scanco software. The number of voxel counts per diameter bin was used as a measure of vessel number [25].

2.2 In vitro Construct Preparation & Characterization

MVF growth and the acellular BMP-2 release kinetics of collagen+DCN hydrogels were assessed and compared to collagen alone and to alginate. Collagen gels were made at 3% w/v and buffered with Dulbecco's modified eagle medium (DMEM; ThermoFisher

Scientific; Waltham, MA). Collagen+DCN gels consisted of 3% collagen supplemented with 50 μg/mL DCN as previously described [32]. To prepare alginate hydrogels, RGD-functionalized alginate (FMC BioPolymer; Ewing, NJ) dissolved in αMEM was crosslinked with calcium sulfate for a final concentration of 2% [38].

MVF were isolated as previously described [22]. Briefly, epididymal fat pads were harvested from Lewis rats, minced, and digested with a collagenase solution for 7 minutes at 37 °C. MVF were obtained through selective filtration to retain tissue between 20–200 μm. Tissue was first passed through a 200 μm filter to remove partially undigested adipose tissue; the flow-through was then passed through a 20 μm filter to remove single cells. MVF were suspended at a density of 80,000 fragments/mL in solution prior to gelation.

To assess BMP-2 release kinetics, acellular gels were loaded with 500 ng BMP-2 (n=4/group) by incorporation within solution prior to gelation. Gels were incubated at 37 °C in αMEM (ThermoFisher) supplemented with 10% fetal bovine serum (Atlanta Biologics; Atlanta, GA). Media was collected and replaced at time points up to day 20. BMP-2 present in the collected media was quantified by ELISA according to manufacturer's instructions (R&D Systems, Minneapolis, MN). BMP-2 release was then compared for acellular vs. MVF-containing collagen+DCN hydrogels as above up to day 7 (n=5/group).

MVF growth in collagen+DCN gels ± BMP-2 was assessed at day 7 (n=5/group). MVFcontaining constructs were cultured in αMEM (ThermoFisher) supplemented with 10% fetal bovine serum (Atlanta Biologics) and 1% penicillin-streptomycin-glutamine (ThermoFisher). In the BMP-2 containing group, 500 ng BMP-2 was incorporated into the collagen+DCN solution prior to gelation. Gels were fixed with 4% paraformaldehyde and stained with rhodamine-labeled Griffonia simplicifolia (GS-1) lectin (Vector Laboratories, Burlingame, CA). Five randomly selected fields were imaged per gel to a depth of 402 μm using a Zeiss LSM 700 confocal microscope. Maximum intensity z-projections were created for each stack, thresholded, and skeletonized using the AngioAnalyzer ImageJ plugin to determine branch number and total length [25, 32].

2.3 Bone Regeneration in Composite Injury

2.3.1 Surgical Procedures—Composite defects were made in 13-week-old female Lewis rats for syngeneic implantation of MVF harvested from Lewis rats. Lewis rats that ubiquitously express GFP (LEW-Tf(CAGEGFP)YsRrrc) were obtained from the Rat Resource and Research Center (RRRC, Columbia, MO) to enable the detection of implanted MVF. Bone defects received either collagen+DCN loaded with 2.5 μg BMP-2 and MVF (BMP-2+MVF), collagen+DCN loaded with BMP-2 (BMP-2), or an empty collagen+DCN gel (gel only). Gels were formed in custom polycarbonate molds to achieve a diameter of 5 mm and a length of 1 cm and placed inside perforated PCL mesh tubes for implantation. 36 animals were used to evaluate the effect of MVF on BMP-2-mediated revascularization and subsequent bone healing. A subset of animals (n=6/BMP-containing group) were euthanized at 7 days post-surgery to assess vascularization using μCT angiography. The remaining animals (n=9/BMP-containing group, n=6/gel only group) were euthanized at 12 weeks post-surgery to assess bone regeneration.

2.3.2 μCT Angiography—For the bone regeneration study, μCT angiography was performed as in 2.1.2 for the early revascularization study; however, all angiography scans were performed at a 15 μm voxel size.

2.3.3 Bone Regeneration Analysis—Bone tissue regeneration was assessed by radiography at 2, 4, 8, and 12 weeks post-surgery and by μCT at 4, 8, and 12 weeks post-surgery. For quantitative μCT analysis, the defect region was scanned with a voxel size of 38 μm. The middle 6.5 mm of the defect was analyzed, and bone volume was quantified by Scanco software using a threshold corresponding to 50% of intact cortical bone [39]. Functional regeneration was assessed by mechanical testing at 12 weeks endpoint. Thighs were harvested, soft tissue was cleared, and fixation plates were removed. Femur ends were potted in Wood's metal (Alfa Aesar) and tested in torsion at a rate of 3°/s to failure or to 30° of rotation (ELF 3200, TA ElectroForce) [37]. The failure strength (torque at failure) and stiffness (linear region of torque vs. rotation plot) were calculated for all samples.

2.3.4 Histology and Immunohistochemistry—Bone tissue was decalcified, sectioned at a 5 μm thickness, and stained with hematoxylin and eosin (H&E; Histotox Labs; Boulder, CO). Immunohistochemistry was also performed on bone tissue sections to evaluate the presence of implanted GFP-expressing MVF. Deparaffinized sections were blocked, incubated with anti-GFP antibody (ab290, Abcam; Cambridge, UK) at a dilution of 1:100, washed, incubated with secondary antibody (A-11036, ThermoFisher) at a dilution of 1:50, washed, and counterstained with DAPI (ThermoFisher) at a dilution of 1:1000.

2.4 Statistical Analysis

Data were analyzed using GraphPad Prism 5, and all statistical tests were conducted with $\alpha=0.05$. BMP-2 release data were analyzed with a repeated measures one-way ANOVA with Bonferroni's multiple comparisons test. MVF network length and branching with and without BMP-2 were compared with a student's t-test with Welch's correction for unequal variances. For the early revascularization study, total vascular volume μCT angiography data were analyzed with a two-way ANOVA with Bonferroni's multiple comparisons test. For the bone healing study, total vascular volume data were analyzed with a one-way ANOVA (thigh) with Bonferroni's multiple comparisons test or with a student's t-test (bone defect area). Vessel thickness histograms were compared using a two-way ANOVA [25] with Bonferroni's multiple comparisons test. Longitudinal bone healing and mechanical testing had significantly different variances among treatment groups (Bartlett's test, $p<0.05$) and were therefore analyzed with Kruskal-Wallis tests and Dunn's multiple comparisons test. Data are plotted as mean with standard error of the mean (SEM) or as a box plot with whiskers indicating the minimum and the maximum.

3. RESULTS

3.1 Early Revascularization Following Composite Injury

To assess the effect of concomitant muscle loss on early revascularization following injury, μCT angiography was used to compare the composite defect to the bone only defect. The total vascular volume of the entire thigh of the bone only defect group was significantly

greater than that of the composite defect group (ANOVA, $p<0.05$) and the contralateral control limb at day 3 ($p<0.01$; Figure 1). The total thigh vascular volume of the bone only defect group was significantly greater than that of the contralateral control limb at day 7 ($p<0.001$), whereas the composite defect thigh vascular volume was not different than that of the contralateral. By day 14, the total thigh vascular volume for both bone only and composite injuries was greater than the contralateral vascular volume ($p<0.001$). The total vascular volume of the bone defect region was not significantly different for composite vs. bone only defects at any time point (Figure 2). Qualitatively, the μCT angiography reconstruction of the composite defect group at day 14 appears asymmetric. Vessels appear to migrate into the defect preferentially from one side of the defect, with the reduced migration side corresponding to the muscle defect. This is particularly evident in the axial view, where vessels can be observed migrating through the perforations in the PCL mesh tube.

In addition to total vascular volume, the distribution of vessel thicknesses was also quantified by examining the number of voxels (counts) per diameter bin. At day 3, the thigh region of the composite defect group had significantly fewer vessels than the bone only defect group (2-way ANOVA, overall effect $p<0.0001$ no significant (n.s.) interaction effect). The thickness distribution within the bone defect region was not significantly different at day 3 (Figure 3 B). At day 7, both the thigh region and bone defect region of the composite defect group had significantly fewer vessels (Figure 3 C-D). The bone defect region had fewer vessels (overall effect $p<0.05$, n.s. interaction effect), and the thigh region specifically had fewer thin vessels under 700 μm in diameter (overall effect $p<0.05$, interaction effect $p<0.05$; Figure 3 C-D). By day 14, both groups exhibited robust vascularization, and the thigh regions showed similar thickness distributions. At the 14 day time point, the composite defect actually exhibited a significantly higher number of vessels within the defect area (overall effect $p<0.01$, n.s. interaction effect).

3.2 In vitro Biomaterial Characterization

Based on the reduced vascularization of composite defects compared to bone only defects observed with μCT angiography, MVF were investigated as a vascular therapeutic for composite injuries. Three different materials were tested in vitro: RGD-alginate, collagen, and collagen+DCN. However, MVF did not sprout or form networks in RGD-alginate, the biomaterial used in the early μCT angiography studies (Figure 4 A). MVF growth was not different in collagen vs. collagen+DCN and robust in both groups (Figure 4 B-C) [32].

Acellular hydrogels were then tested for BMP-2 release. Collagen+DCN released significantly less BMP-2 over days 1–5 than either collagen alone or alginate. By day 10, collagen+DCN released less BMP-2 than collagen alone but was not statistically different than alginate. At days 15–20, the quantity of BMP-2 released by all three materials was significantly different (Figure 4 D; RM-ANOVA, $p<0.05$). At day 20, collagen had released about 35% of the loaded BMP-2, collagen+DCN had released about 28%, and alginate had released about 25%.

Release of BMP-2 from acellular vs. MVF-containing collagen+DCN gels was compared up to day 7. Beginning at day 3, the MVF-containing gels released significantly more BMP-2

than acellular gels (Figure 5 A; RM-ANOVA, $p<0.05$). This difference persisted through day 7 ($p<0.01$). At day 7, MVF-containing gels had released 12.9% of the loaded BMP-2, and acellular gels had released 11.6%. BMP-2 significantly increased total MVF network length and branching (Figure 5 B) and qualitatively appeared to accelerate MVF network formation (Figure 5 C-D).

3.3 Effect of MVF on Early Revascularization Following Composite Injury

Composite defects were treated with either collagen+DCN gels loaded with BMP-2 and MVF, collagen+DCN gels loaded with BMP-2 alone, or empty collagen+DCN gels only. Based on the reduced number of small diameter vessels within both the thigh and bone defect region at day 7 of the early revascularization study, 6 animals per BMP-containing treatment group were euthanized 7 days post-surgery for μCT angiography.

Both treatment groups had significantly greater thigh vascular volume than the contralateral leg (Figure 6 A-B; $p<0.0001$). However, the total vascular volume was not significantly different between BMP and BMP+MVF in the thigh region or the bone defect region. Analysis of vessel size distributions revealed that compared to BMP alone, BMP+MVF treated defects had significantly fewer vessels in the bone defect regions (Figure 6 C; 2-way ANOVA, overall effect $p<0.01$, n.s. interaction effect). The thigh region possessed fewer small diameter vessels, ranging 0–200 μm and 600–1000 μm in the BMP+MVF animals compared to the BMP animals (overall effect $p<0.0001$, interaction effect $p<0.01$).

3.4 Effect of MVF on Bone Regeneration in Composite Injury

At 12 weeks, radiography demonstrated inconsistent bridging in both BMP-containing groups (with and without MVF; Figure 7). Semi-quantitative bridging scores 0–4 were assigned to each animal: 0, no mineralization; 1, sparse, isolated areas of mineral; 2, substantial but discontinuous mineralization; 3, near but incomplete bridging; 4, complete bridging [40]. Both BMP-containing groups had approximately one third of defects completely bridge (score 4), one third produce substantial mineralization without bridging (score 2–3), and one third with little to no mineral (score 0–1). The gel only control group did not induce substantial bone formation in any animal (all scored 0–1).

Bone volume as measured by μCT was significantly higher in both BMP-containing groups than the gel only control at 12 weeks (Kruskal-Wallis test, $p=0.011$; Figure 8 A); there was no effect of MVF on bone volume. There was no difference among treatment groups in failure strength or stiffness, and all groups were significantly below that of the intact contralateral control (KruskalWallis test, $p<0.001$; Figure 8 B-C).

3.5.1 Histology—H&E staining demonstrated that even in samples with moderate bone volume, the defect area often failed to bridge with one or both intact bone ends (Figure 9 A); this is in agreement with the radiography shown in Figure 7. Due to the high variability of bone volume, H&E was performed on three samples representing low, moderate, and high bone volume for each treatment group (the collagen+DCN gel only group only produced low bone volume, so only one sample was stained; Figure 9). The low bone volume samples displayed primarily fibrous tissue. The low bone volume samples from the BMP-containing

groups appeared more loosely structured than the gel only group, which was very densely cellular. The moderate bone volume samples appeared to have islands of mineralized tissue within larger areas of marrow-like tissue. The high bone volume samples had fewer and smaller areas of marrow-like tissue. Although there were larger areas of mineralized tissue, they appear more disorganized than intact mature bone tissue.

3.5.2 Immunohistochemistry—Immunohistochemistry was performed to determine whether the implanted GFP-expressing MVF remained within the defect at either 1 week or 12 weeks post-surgery. At 1 week, GFP+cells were identifiable in the defect region (Figure 10); however, rather than being evenly distributed throughout the defect, these GFP+ cells appeared to be clustered together. Additionally, they appeared as distinct, single cells rather than multicellular vessel structures and are not associated with vascular structures. At week 12, no cells stained positive for GFP.

4. DISCUSSION

A key indicator of traumatic composite injury severity is vascular integrity [3]. Clinically, bone injuries with concomitant muscle damage are more prone to complications and long-term disability, and those with vascular damage are the most susceptible [1, 2]. We have previously developed a rat model of composite injury that recapitulates the bone healing deficit seen clinically [4]; however, the vascularization response had not yet been investigated. Here, our hypothesis that revascularization following injury is impaired in the composite defect relative to the bone only defect was supported. Our hypotheses that the addition of MVF as a vascular therapeutic would improve early revascularization of the composite defect and subsequent BMP-2-mediated bone healing were not supported.

Revascularization following injury was impaired in the composite defect relative to the bone only defect. At day 3 post-surgery, the bone defect only group had a significantly higher thigh vascular volume than the contralateral limb, indicating the vascular ingrowth stage of the wound healing cascade had initiated. The bone defect only group also had significantly higher thigh vascular volume than the composite defect group, suggesting a delayed revascularization response in the composite model. At day 3, both bone defect regions showed a comparably sparse revascularization. The reduced vascularity of the thigh, which encompasses both bone and muscle tissue, in the composite group may possibly be due to the frank loss of muscle tissue and its associated vascular supply. However, at day 7, both the thigh and the bone defect area of the composite group showed a reduced number of vessels compared to bone injury alone. Due to the lack of surrounding soft tissue, vascular ingrowth may have been required to traverse a greater distance and was thus unable to reach the bone defect by day 7. By day 14, the thigh regions exhibited similarly robust vascularization, with both defect groups having significantly greater total volume than the contralateral. Within the bone defect area, the composite group actually had a greater number of small vessels under 200 μm in diameter but none of the larger vessels 450–700 μm as seen in bone only group. This altered vessel size distribution profile may indicate delayed revascularization; the bone-only injuries may have remodeled the initial network into larger diameter vessels by day 14, whereas the composite defect was just beginning to form small vessels. While the total vascular volume within the bone defect was not

significantly different between groups at any time point, the significant differences in size distribution suggest differences in vascular network maturity. While we have not shown a direct, causal relationship between altered revascularization and impaired bone healing, previous studies that inhibited vascularization resulted in delayed union [8]. Taken together with existing literature, this study suggests that the impaired early revascularization timeline seen here in the composite defect model may contribute to the attenuated bone healing observed downstream – either directly or indirectly. The impaired vascularization response may impede the regenerative processes of progenitor cell recruitment and differentiation and instead lead to a more inflammatory and fibrotic response [5]. However, previous work has shown that reduced blood flow associated with a muscle crush injury did not impair fracture healing [41].

In an effort to rescue this vascular deficit, collagen+DCN hydrogels were developed as a biomaterial delivery vehicle for both BMP-2 and MVF. This material has previous been shown to support vascular growth in vitro with minimal cell-mediated contraction of the gel [32]. Similar vascularized constructs have been implanted and progressed to connect with the host vasculature [24], increase tissue vascular volume [25], and respond to local microenvironmental characteristics [23]. However, in this application, MVF were not able to overcome the vascular deficit and in fact were associated with decreased number of vessels relative to BMP alone at day 7. The timing of VEGF expression has been implicated as an important regulator of bone healing [16, 17], and delivering MVF immediately following injury may have disrupted the endogenous timeline of wound healing angiogenesis. Endogenous VEGF expression typically peaks around day 5–10 post-injury [17], while delivering MVF immediately following defect creation may have introduced larger amounts of VEGF much earlier. Early presence of VEGF may have then disrupted growth factor gradients and prevented the full endogenous angiogenic response. However, a majority of BMP-2 and VEGF co-delivery studies that ultimately did not show improved bone healing did observe increased vascularity [15–18, 26]. A previous study examining the effect of hindlimb ischemia on segmental defect healing observed a beneficial effect of transient ischemia on revascularization and subsequent bone healing [42]; the complexity of the relationship between vascularization and bone regeneration is not yet fully understood. Although GFP+ cells were observed within the defect area at day 7, they appeared as single cells rather than the GFP+ multicellular vessel fragments that were implanted. While some loss of support cells is a normal element of sprouting angiogenesis, the GFP+ cells do not appear to be associated with vessel-like structures, suggesting instead that a majority of the cells comprising the MVF dissociated to a single cell level. As the implanted vessel fragments dissociated, vessel destabilization cues may possibly have been transmitted to the surrounding tissue, resulting in a decreased number of vessels within the thigh compared to BMP alone. Previous studies delivering MVF that showed increased tissue vascular volume had pre-cultured the MVF in vitro prior to implantation, which allowed for provisional network formation [25]. While the freshly isolated MVF tested in this study potentially have greater translational applicability, the pre-culture of constructs accelerates inosculation [43] and may be critical to functional revascularization by implanted cells.

MVF also did not have a statistically significant effect on bone volume or mechanical properties. However, the mean and median bone volume, failure strength, and torsional

stiffness were all lower in the BMP-2 + MVF group than in the BMP-2 alone group. This may primarily be due to their negative effect on the already dampened revascularization response in the composite defect model. GFP+ MVF-derived cells were not observed in the defect tissue at the 12 week end point, indicating that they did not integrate into the regenerated tissue. Cell-based therapies broadly are challenged by issues of retention and survival [44, 45]; although the implanted cells in this study were able to persist to day 7, without inosculating with the host vasculature, they may have failed to survive within the harsh, hypoxic injury environment. Additionally, exogenous cells may metabolize or degrade BMP-2, thereby reducing its effective dose and availability to osteoprogenitors [46]. However, the in vitro BMP-2 release experiment showed that MVF-containing collagen +DCN gels released modestly but significantly more detectable BMP-2 than acellular gels. This may be due to proteolytic activity of MVF as they sprout and invade the matrix. BMP-2 also significantly increased MVF network length and branching at day 7, which is in agreement with previous reports of BMP-2 increasing angiogenesis [47, 48]. Previous literature showed decreased mineralization when adipose-derived MSCs were co-delivered with BMP-2, whereas bone marrow-derived MSCs increased BMP-2-mediated mineralization [49]. While adipose-derived MVF do contain MSCs, they represent only about 5% of the cellular constituents [50, 51]. Cell source more broadly may be an important consideration when using MVF therapeutically. Further, even in samples with moderate bone volume, the defect area often failed to bridge with one or both intact bone ends across both BMP-containing treatment groups. While we have established an association between altered revascularization and impaired bone healing, other factors may also contribute to reduced healing. There is evidence for crosstalk between growth factors secreted by muscle tissue and the periosteum [4], perhaps contributing for the relatively low bridging rates observed in this study. The loss of adjacent muscle tissue sustains the pro-inflammatory stage of wound healing [5], and immunomodulatory agents have been shown to improve bone healing in traumatic injuries with volumetric muscle loss [52]. Composite tissue injuries are complex and may require adjunct therapies to address multiple facets of the healing process.

The collagen+DCN delivery vehicle met the in vitro design criteria as a matrix supporting both MVF growth and sustained BMP-2 delivery. MVF grow robustly in collagen+DCN [32], and DCN increased the retention of BMP-2 in vitro compared to collagen alone. At an intermediate timepoint (day 10 of 20), the BMP-2 release of collagen+DCN was not statistically different than alginate. DCN preferentially binds TGF-ß family growth factors such as BMP-2 [36]. As such, DCN may have transiently bound BMP-2, increasing retention, and released it, allowing BMP-2-induced mineralization [35]. Interestingly, DCN has been shown to play a role in angiogenesis, with studies showing both positive and negative effects [53–57]. DCN deficient mice exhibit deficiencies in angiogenesis [58], and sprouting endothelial cells express DCN [59]. As an extracellular matrix component, DCN has been shown to inhibit endothelial cell tube formation [53]. However, collagen+DCN is an effective in vitro culture substrate for MVF and facilitates network branching and extension [32]. Collagen+DCN supports angiogenesis in vivo as well. Vessels were able to migrate into the bone defect area, and the 7 day perfusion results appeared qualitatively similar to those observed at day 7 in the alginate system.

As a delivery vehicle for BMP-2, collagen+DCN gels are capable of bridging the challenging composite defect model, albeit inconsistently; mineralization occurred in approximately twothirds of BMP-treated defects. A previous study of bone healing in the composite defect model observed very comparable bone volume and mechanical properties in composite defects using a well-established alginate delivery vehicle for a functionally equivalent dose of BMP-2 (2 vs. 2.5 μg) [4]. In the present study, the average 12 week bone volume of the BMP only group was 33.38 mm^3, and the average failure strength was 0.0779 Nm; Willett et al. observed a 12 week bone volume of 28.99 mm^3 and a failure strength of 0.0558 Nm in composite defects treated with BMP-2 delivered in alginate. Thus, the inconsistent bone healing observed here may speak more to the extraordinarily challenging nature of composite tissue injuries rather than the efficacy of collagen+DCN as a BMP-2 delivery vehicle. Although not able to promote consistent bridging in challenging composite tissue injuries, collagen+DCN performed as well as RGD-alginate as a vehicle for sustained delivery of BMP-2.

5. CONCLUSIONS

Composite injuries to bone and adjacent soft tissue are more prone to clinical complications and poor healing outcomes. In an established rat bone-muscle injury model, this study demonstrated a modest but significant impairment in early revascularization, which may contribute to impaired bone healing. In an attempt to overcome this vascular deficit, we developed and characterized collagen+DCN hydrogels as a co-delivery vehicle for a vascular therapeutic, MVF, and the osteoinductive growth factor, BMP-2. However, despite in vitro data suggesting synergistic effects between BMP-2 and MVF, we unexpectedly found that MVF did not increase vascular volume and in fact decreased the number of vessels both within the bone defect area and the surrounding tissues of the thigh. GFP+ cells from the implanted GFP+ MVF were present within the bone defect at 1 week post-surgery but appeared as single cells rather than as vessel structures, and no GFP+ cells were observed at 12 weeks post-surgery. Although MVF did not improve bone healing, the collagen+DCN biomaterial delivery of BMP-2 was able to achieve bridging in the challenging composite defect model, reaching endpoint bone volume and mechanical properties comparable to a well-established RGD-alginate delivery system. Decorin-supplemented collagen hydrogel is therefore a promising biomaterial delivery vehicle for treating composite extremity injuries, and future studies will explore pre-culturing MVF in vitro to allow stable network formation prior to implantation.

ACKNOWLEDGEMENTS

This work was supported by funding from the National Institutes of Health (NIH) R01 AR069297 and from the Armed Forces Institute for Regenerative Medicine (AFIRM II) effort under award number W81XWH-14-2-0003. Opinions, interpretations, conclusions, and recommendations are those of the authors and are not necessarily endorsed by the Department of Defense. The authors wish to acknowledge the core facilities at the Parker H. Petit Institute for Bioengineering and Bioscience at the Georgia Institute of Technology for the use of their shared equipment, services, and expertise. We also thank Ryan Akman, Shannon Anderson, Fabrice Bernard, Gilad Doron, Emily Eastburn, Brett Klosterhoff, Angela Lin, Giuliana Salazar-Noratto, Ramesh Subbiah, and Casey Vantucci for their assistance with surgeries.

7. REFERENCES

[1]. Zura R, Xiong Z, Einhorn T, Watson JT, Ostrum RF, Prayson MJ, Della Rocca GJ, Mehta S, McKinley T, Wang Z, Steen RG, Epidemiology of Fracture Nonunion in 18 Human Bones, JAMA Surg 151(11) (2016) e162775. [PubMed: 27603155]

[2]. MacKenzie EJ, Bosse MJ, Pollak AN, Webb LX, Swiontkowski MF, Kellam JF, Smith DG, Sanders RW, Jones AL, Starr AJ, McAndrew MP, Patterson BM, Burgess AR, Castillo RC, Long-term persistence of disability following severe lower-limb trauma. Results of a seven-year follow-up, J Bone Joint Surg Am 87(8) (2005) 1801–9. [PubMed: 16085622]

[3]. Gustilo RB, Merkow RL, Templeman D, The management of open fractures, J Bone Joint Surg Am 72(2) (1990) 299–304. [PubMed: 2406275]

[4]. Willett NJ, Li MT, Uhrig BA, Boerckel JD, Huebsch N, Lundgren TL, Warren GL, Guldberg RE, Attenuated human bone morphogenetic protein-2-mediated bone regeneration in a rat model of composite bone and muscle injury, Tissue engineering. Part C, Methods 19(4) (2013) 316–25. [PubMed: 22992043]

[5]. Hurtgen BJ, Ward CL, Garg K, Pollot BE, Goldman SM, McKinley TO, Wenke JC, Corona BT, Severe muscle trauma triggers heightened and prolonged local musculoskeletal inflammation and impairs adjacent tibia fracture healing, J Musculoskelet Neuronal Interact 16(2) (2016) 122–34. [PubMed: 27282456]

[6]. Pollot BE, Goldman SM, Wenke JC, Corona BT, Decellularized extracellular matrix repair of volumetric muscle loss injury impairs adjacent bone healing in a rat model of complex musculoskeletal trauma, J Trauma Acute Care Surg 81(5 Suppl 2 Proceedings of the 2015 Military Health System Research Symposium) (2016) S184–S190. [PubMed: 27533905]

[7]. Einhorn TA, Gerstenfeld LC, Fracture healing: mechanisms and interventions, Nat Rev Rheumatol 11(1) (2015) 45–54. [PubMed: 25266456]

[8]. Lu C, Miclau T, Hu D, Marcucio RS, Ischemia leads to delayed union during fracture healing: a mouse model, Journal of orthopaedic research : official publication of the Orthopaedic Research Society 25(1) (2007) 51–61. [PubMed: 17019699]

[9]. Hyzy SL, Kajan I, Wilson DS, Lawrence KA, Mason D, Williams JK, Olivares-Navarrete R, Cohen DJ, Schwartz Z, Boyan BD, Inhibition of angiogenesis impairs bone healing in an in vivo murine rapid resynostosis model, Journal of biomedical materials research. Part A 105(10) (2017) 2742–2749. [PubMed: 28589712]

[10]. Liu C, Castillo AB, Targeting Osteogenesis-Angiogenesis Coupling for Bone Repair, J Am Acad Orthop Surg 26(7) (2018) e153–e155. [PubMed: 29489598]

[11]. Krishnan L, Willett NJ, Guldberg RE, Vascularization strategies for bone regeneration, Annals of biomedical engineering 42(2) (2014) 432–44. [PubMed: 24468975]

[12]. Zhang W, Zhu C, Wu Y, Ye D, Wang S, Zou D, Zhang X, Kaplan DL, Jiang X, VEGF and BMP-2 promote bone regeneration by facilitating bone marrow stem cell homing and differentiation, Eur Cell Mater 27 (2014) 1–11;

[13]. Peng H, Usas A, Olshanski A, Ho AM, Gearhart B, Cooper GM, Huard J, VEGF improves, whereas sFlt1 inhibits, BMP-2-induced bone formation and bone healing through modulation of angiogenesis, Journal of bone and mineral research : the official journal of the American Society for Bone and Mineral Research 20(11) (2005) 2017–27.

[14]. Subbiah R, Hwang MP, Van SY, Do SH, Park H, Lee K, Kim SH, Yun K, Park K, Osteogenic/angiogenic dual growth factor delivery microcapsules for regeneration of vascularized bone tissue, Adv Healthc Mater 4(13) (2015) 1982–92. [PubMed: 26138344]

[15]. Geuze RE, Theyse LF, Kempen DH, Hazewinkel HA, Kraak HY, Oner FC, Dhert WJ, Alblas J, A differential effect of bone morphogenetic protein-2 and vascular endothelial growth factor release timing on osteogenesis at ectopic and orthotopic sites in a large-animal model, Tissue engineering. Part A 18(19–20) (2012) 2052–62. [PubMed: 22563713]

[16]. Hernandez A, Reyes R, Sanchez E, Rodriguez-Evora M, Delgado A, Evora C, In vivo osteogenic response to different ratios of BMP-2 and VEGF released from a biodegradable porous system, Journal of biomedical materials research. Part A 100(9) (2012) 2382–91. [PubMed: 22528545]

[17]. Kempen DH, Lu L, Heijink A, Hefferan TE, Creemers LB, Maran A, Yaszemski MJ, Dhert WJ, Effect of local sequential VEGF and BMP-2 delivery on ectopic and orthotopic bone regeneration, Biomaterials 30(14) (2009) 2816–25. [PubMed: 19232714]

[18]. Patel ZS, Young S, Tabata Y, Jansen JA, Wong ME, Mikos AG, Dual delivery of an angiogenic and an osteogenic growth factor for bone regeneration in a critical size defect model, Bone 43(5) (2008) 931–40. [PubMed: 18675385]

[19]. Seebach C, Henrich D, Kahling C, Wilhelm K, Tami AE, Alini M, Marzi I, Endothelial progenitor cells and mesenchymal stem cells seeded onto beta-TCP granules enhance early vascularization and bone healing in a critical-sized bone defect in rats, Tissue engineering. Part A 16(6) (2010) 1961–70. [PubMed: 20088701]

[20]. Yu H, VandeVord PJ, Mao L, Matthew HW, Wooley PH, Yang SY, Improved tissue-engineered bone regeneration by endothelial cell mediated vascularization, Biomaterials 30(4) (2009) 508–17. [PubMed: 18973938]

[21]. Tsigkou O, Pomerantseva I, Spencer JA, Redondo PA, Hart AR, O'Doherty E, Lin Y, Friedrich CC, Daheron L, Lin CP, Sundback CA, Vacanti JP, Neville C, Engineered vascularized bone grafts, Proceedings of the National Academy of Sciences of the United States of America 107(8) (2010) 3311–6. [PubMed: 20133604]

[22]. Hoying JB, Boswell CA, Williams SK, Angiogenic potential of microvessel fragments established in three-dimensional collagen gels, In vitro cellular & developmental biology. Animal 32(7) (1996) 409–19.

[23]. Chang CC, Krishnan L, Nunes SS, Church KH, Edgar LT, Boland ED, Weiss JA, Williams SK, Hoying JB, Determinants of microvascular network topologies in implanted neovasculatures, Arteriosclerosis, thrombosis, and vascular biology 32(1) (2012) 5–14.

[24]. Nunes SS, Greer KA, Stiening CM, Chen HY, Kidd KR, Schwartz MA, Sullivan CJ, Rekapally H, Hoying JB, Implanted microvessels progress through distinct neovascularization phenotypes, Microvascular research 79(1) (2010) 10–20. [PubMed: 19833141]

[25]. Li MT, Ruehle M, Stevens H, Servies N, Willett N, Karthikeyakannan S, Warren GL, Guldberg R, Krishnan LN, Skeletal myoblast-seeded vascularized tissue scaffolds in the treatment of a large volumetric muscle defect in the rat biceps femoris muscle, Tissue engineering. Part A (2017).

[26]. Garcia JR, Clark AY, Garcia AJ, Integrin-specific hydrogels functionalized with VEGF for vascularization and bone regeneration of critical-size bone defects, Journal of biomedical materials research. Part A 104(4) (2016) 889–900. [PubMed: 26662727]

[27]. Park JY, Shim JH, Choi SA, Jang J, Kim M, Lee SH, Cho DW, 3D printing technology to control BMP-2 and VEGF delivery spatially and temporally to promote large-volume bone regeneration, J Mater Chem B 3(27) (2015) 5415–5425.

[28]. Krishnan L, Priddy LB, Esancy C, Klosterhoff BS, Stevens HY, Tran L, Guldberg RE, Delivery vehicle effects on bone regeneration and heterotopic ossification induced by high dose BMP-2, Acta biomaterialia 49 (2017) 101–112. [PubMed: 27940197]

[29]. Kolambkar YM, Boerckel JD, Dupont KM, Bajin M, Huebsch N, Mooney DJ, Hutmacher DW, Guldberg RE, Spatiotemporal delivery of bone morphogenetic protein enhances functional repair of segmental bone defects, Bone 49(3) (2011) 485–92. [PubMed: 21621027]

[30]. Edgar LT, Hoying JB, Utzinger U, Underwood CJ, Krishnan L, Baggett BK, Maas SA, Guilkey JE, Weiss JA, Mechanical interaction of angiogenic microvessels with the extracellular matrix, Journal of biomechanical engineering 136(2) (2014)

[31]. Krishnan L, Hoying JB, Nguyen H, Song H, Weiss JA, Interaction of angiogenic microvessels with the extracellular matrix, American journal of physiology. Heart and circulatory physiology 293(6) (2007) H3650–8. [PubMed: 17933969]

[32]. Ruehle MA, Krishnan L, LaBelle SA, Willett NJ, Weiss JA, Guldberg RE, Decorin-containing collagen hydrogels as dimensionally stable scaffolds to study the effects of compressive mechanical loading on angiogenesis, MRS Communications 7(3) (2017) 466–471. [PubMed: 29450108]

[33]. Matuszewski PE, Chen YL, Szczesny SE, Lake SP, Elliott DM, Soslowsky LJ, Dodge GR, Regional variation in human supraspinatus tendon proteoglycans: decorin, biglycan, and aggrecan, Connect Tissue Res 53(5) (2012) 343–8. [PubMed: 22329809]

[34]. Reese SP, Underwood CJ, Weiss JA, Effects of decorin proteoglycan on fibrillogenesis, ultrastructure, and mechanics of type I collagen gels, Matrix Biol 32(7–8) (2013) 414–23. [PubMed: 23608680]

[35]. Ferdous Z, Wei VM, Iozzo R, Hook M, Grande-Allen KJ, Decorin-transforming growth factor-interaction regulates matrix organization and mechanical characteristics of three-dimensional collagen matrices, J Biol Chem 282(49) (2007) 35887–98. [PubMed: 17942398]

[36]. Hildebrand A, Romaris M, Rasmussen LM, Heinegard D, Twardzik DR, Border WA, Ruoslahti E, Interaction of the small interstitial proteoglycans biglycan, decorin and fibromodulin with transforming growth factor beta, Biochem J 302 (Pt 2) (1994) 527–34. [PubMed: 8093006]

[37]. Oest ME, Dupont KM, Kong HJ, Mooney DJ, Guldberg RE, Quantitative assessment of scaffold and growth factor-mediated repair of critically sized bone defects, Journal of orthopaedic research : official publication of the Orthopaedic Research Society 25(7) (2007) 941–50. [PubMed: 17415756]

[38]. Kolambkar YM, Dupont KM, Boerckel JD, Huebsch N, Mooney DJ, Hutmacher DW, Guldberg RE, An alginate-based hybrid system for growth factor delivery in the functional repair of large bone defects, Biomaterials 32(1) (2011) 65–74. [PubMed: 20864165]

[39]. Boerckel JD, Kolambkar YM, Dupont KM, Uhrig BA, Phelps EA, Stevens HY, Garcia AJ, Guldberg RE, Effects of protein dose and delivery system on BMP-mediated bone regeneration, Biomaterials 32(22) (2011) 5241–51. [PubMed: 21507479]

[40]. Sarkar MR, Augat P, Shefelbine SJ, Schorlemmer S, Huber-Lang M, Claes L, Kinzl L, Ignatius A, Bone formation in a long bone defect model using a platelet-rich plasma-loaded collagen scaffold, Biomaterials 27(9) (2006) 1817–23. [PubMed: 16307796]

[41]. Utvag SE, Grundnes O, Rindal DB, Reikeras O, Influence of extensive muscle injury on fracture healing in rat tibia, Journal of orthopaedic trauma 17(6) (2003) 430–5. [PubMed: 12843728]

[42]. Uhrig BA, Boerckel JD, Willett NJ, Li MT, Huebsch N, Guldberg RE, Recovery from hind limb ischemia enhances rhBMP-2-mediated segmental bone defect repair in a rat composite injury model, Bone 55(2) (2013) 410–7. [PubMed: 23664918]

[43]. Laschke MW, Mussawy H, Schuler S, Kazakov A, Rucker M, Eglin D, Alini M, Menger MD, Short-term cultivation of in situ prevascularized tissue constructs accelerates inosculation of their preformed microvascular networks after implantation into the host tissue, Tissue engineering. Part A 17(5–6) (2011) 841–53. [PubMed: 20973748]

[44]. Levit RD, Landazuri N, Phelps EA, Brown ME, Garcia AJ, Davis ME, Joseph G, Long R, Safley SA, Suever JD, Lyle AN, Weber CJ, Taylor WR, Cellular encapsulation enhances cardiac repair, Journal of the American Heart Association 2(5) (2013) e000367. [PubMed: 24113327]

[45]. Allen AB, Gazit Z, Su S, Stevens HY, Guldberg RE, In vivo bioluminescent tracking of mesenchymal stem cells within large hydrogel constructs, Tissue engineering. Part C, Methods 20(10) (2014) 806–16. [PubMed: 24576050]

[46]. Allen AB, Zimmermann JA, Burnsed OA, Yakubovich DC, Stevens HY, Gazit Z, McDevitt TC, Guldberg RE, Environmental manipulation to promote stem cell survival in vivo: use of aggregation, oxygen carrier, and BMP-2 co-delivery strategies, J Mater Chem B 4(20) (2016) 3594–3607.

[47]. Raida M, Heymann AC, Gunther C, Niederwieser D, Role of bone morphogenetic protein 2 in the crosstalk between endothelial progenitor cells and mesenchymal stem cells, Int J Mol Med 18(4) (2006) 735–9. [PubMed: 16964430]

[48]. Finkenzeller G, Hager S, Stark GB, Effects of bone morphogenetic protein 2 on human umbilical vein endothelial cells, Microvascular research 84(1) (2012) 81–5. [PubMed: 22487440]

[49]. Dosier CR, Uhrig BA, Willett NJ, Krishnan L, Li MT, Stevens HY, Schwartz Z, Boyan BD, Guldberg RE, Effect of cell origin and timing of delivery for stem cell-based bone tissue engineering using biologically functionalized hydrogels, Tissue engineering. Part A 21(1–2) (2015) 156–65. [PubMed: 25010532]

[50]. Frueh FS, Spater T, Lindenblatt N, Calcagni M, Giovanoli P, Scheuer C, Menger MD, Laschke MW, Adipose Tissue-Derived Microvascular Fragments Improve Vascularization, Lymphangiogenesis, and Integration of Dermal Skin Substitutes, J Invest Dermatol 137(1) (2017) 217–227. [PubMed: 27574793]

[51]. Laschke MW, Grasser C, Kleer S, Scheuer C, Eglin D, Alini M, Menger MD, Adipose tissue-derived microvascular fragments from aged donors exhibit an impaired vascularisation capacity, Eur Cell Mater 28 (2014) 287–98. [PubMed: 25340807]

[52]. Hurtgen BJ, Henderson BEP, Ward CL, Goldman SM, Garg K, McKinley TO, Greising SM, Wenke JC, Corona BT, Impairment of early fracture healing by skeletal muscle trauma is restored by FK506, BMC musculoskeletal disorders 18(1) (2017) 253. [PubMed: 28606129]

[53]. Davies Cde L, Melder RJ, Munn LL, Mouta-Carreira C, Jain RK, Boucher Y, Decorin inhibits endothelial migration and tube-like structure formation: role of thrombospondin-1, Microvascular research 62(1) (2001) 26–42. [PubMed: 11421658]

[54]. Fiedler LR, Eble JA, Decorin regulates endothelial cell-matrix interactions during angiogenesis, Cell Adh Migr 3(1) (2009) 3–6. [PubMed: 19372733]

[55]. Grant DS, Yenisey C, Rose RW, Tootell M, Santra M, Iozzo RV, Decorin suppresses tumor cell-mediated angiogenesis, Oncogene 21(31) (2002) 4765–77. [PubMed: 12101415]

[56]. Jarvelainen H, Sainio A, Wight TN, Pivotal role for decorin in angiogenesis, Matrix Biol 43 (2015) 15–26. [PubMed: 25661523]

[57]. Jarvelainen HT, Iruela-Arispe ML, Kinsella MG, Sandell LJ, Sage EH, Wight TN, Expression of decorin by sprouting bovine aortic endothelial cells exhibiting angiogenesis in vitro, Exp Cell Res 203(2) (1992) 395–401. [PubMed: 1281110]

[58]. Schonherr E, Sunderkotter C, Schaefer L, Thanos S, Grassel S, Oldberg A, Iozzo RV, Young MF, Kresse H, Decorin deficiency leads to impaired angiogenesis in injured mouse cornea, J Vasc Res 41(6) (2004) 499–508. [PubMed: 15528932]

[59]. Schonherr E, O'Connell BC, Schittny J, Robenek H, Fastermann D, Fisher LW, Plenz G, Vischer P, Young MF, Kresse H, Paracrine or virus-mediated induction of decorin expression by endothelial cells contributes to tube formation and prevention of apoptosis in collagen lattices, Eur J Cell Biol 78(1) (1999) 44–55. [PubMed: 10082423]

Statement of Significance:

We have previously established a model of musculoskeletal trauma that exhibits impaired bone healing. For the first time, this work shows that the early revascularization response is also significantly, albeit modestly, impaired. A decorin-supplemented collagen hydrogel was used for the first time in vivo as a delivery vehicle for both a cell-based vascular therapeutic, MVF, and an osteoinductive growth factor, BMP-2. While MVF did not improve vascular volume or bone healing, collagen+DCN is a BMP-2 delivery vehicle capable of achieving bridging in the challenging composite defect model. Based on its support of robust angiogenesis in vitro, collagen+DCN may be extended for future use with other vascular therapeutics such as pre-formed vascular networks.

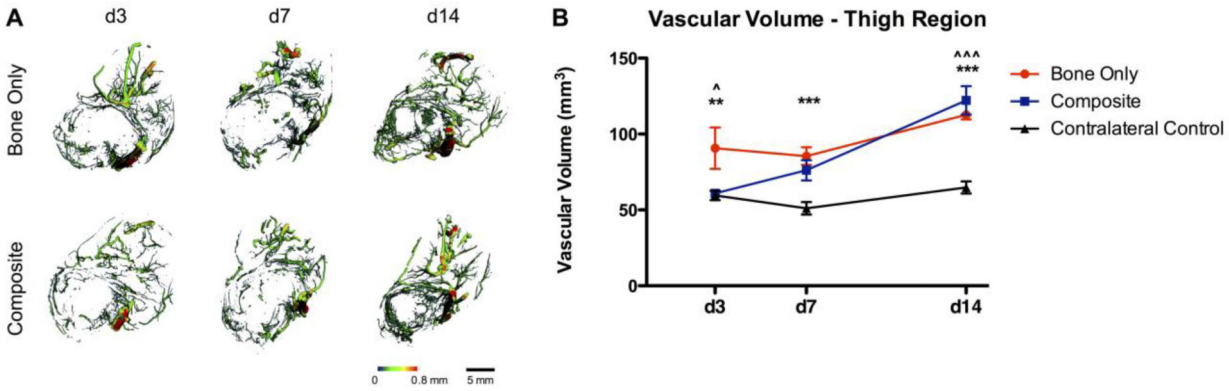

Figure 1.

A) Representative images of vasculature within the thigh region of Bone Only vs Composite injuries at days 3, 7, and 14. Heatmaps correspond to vessel diameter 0–0.8 mm. B) Quantitative μCT angiography results for the thigh region, n=7–9/group. ** $p<0.01$ between Bone Only and Contralateral, *** $p<0.001$ between Bone Only and Contralateral. ^ $p<0.05$ between Composite and Bone Only, ^^^ $p<0.001$ between Composite and Contralateral.

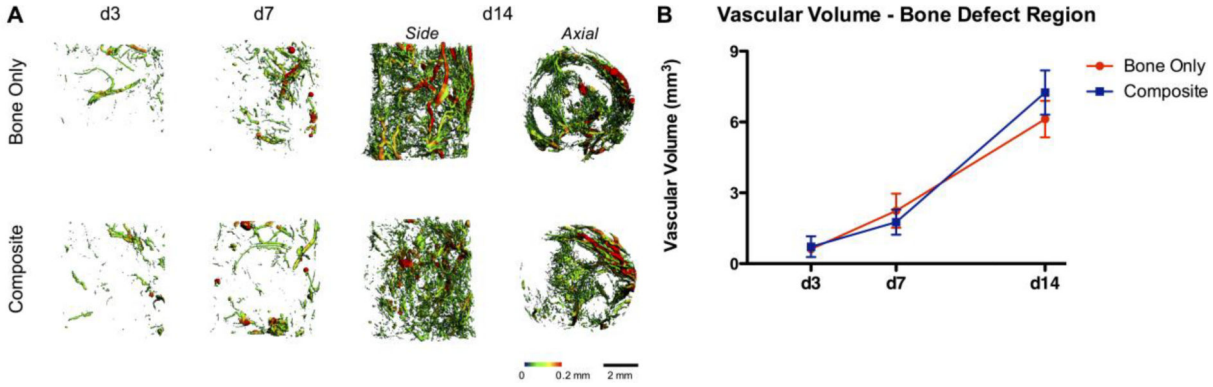

Figure 2.

A) Representative images of vasculature within the bone defect region of Bone Only vs Composite injuries at days 3, 7, and 14. Heatmaps correspond to vessel diameter 0–0.2 mm. B) Quantitative μCT angiography results for total vascular volume of the bone defect region, n=7–9/group.

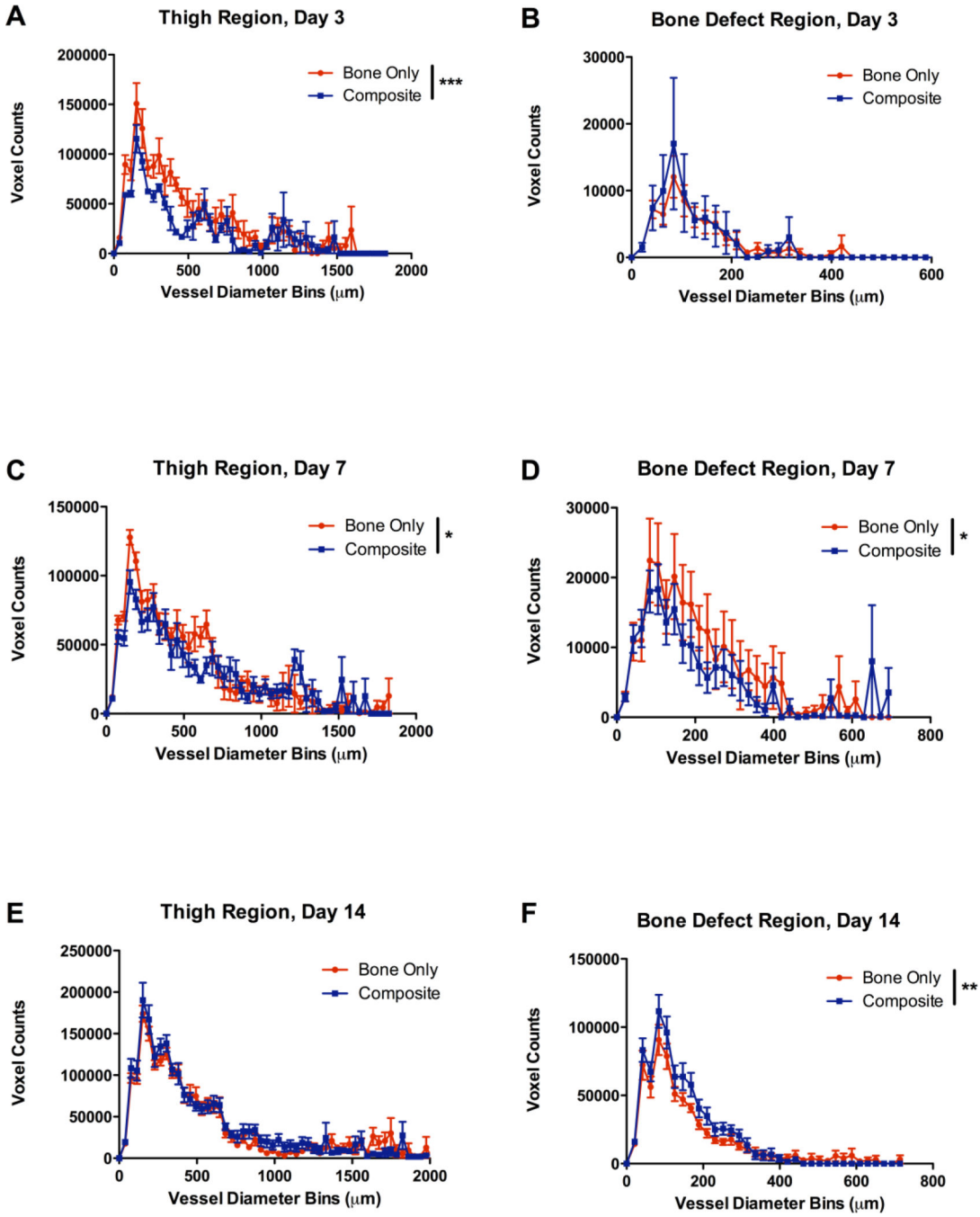

Figure 3.

Vascular thickness distributions for A) the thigh at day 3, B) the bone defect at day 3, C) the thigh at day 7, D) the bone defect at day 7, E) the thigh at day 14, and F) the bone defect at day 14. Voxel counts indicate the number of voxels with a given diameter and are utilized as a measure of vessel number. n=7–9/group, * $p<0.05$ between Bone Only and Composite (overall effect), ** $p<0.01$, ** $p<0.0001$.

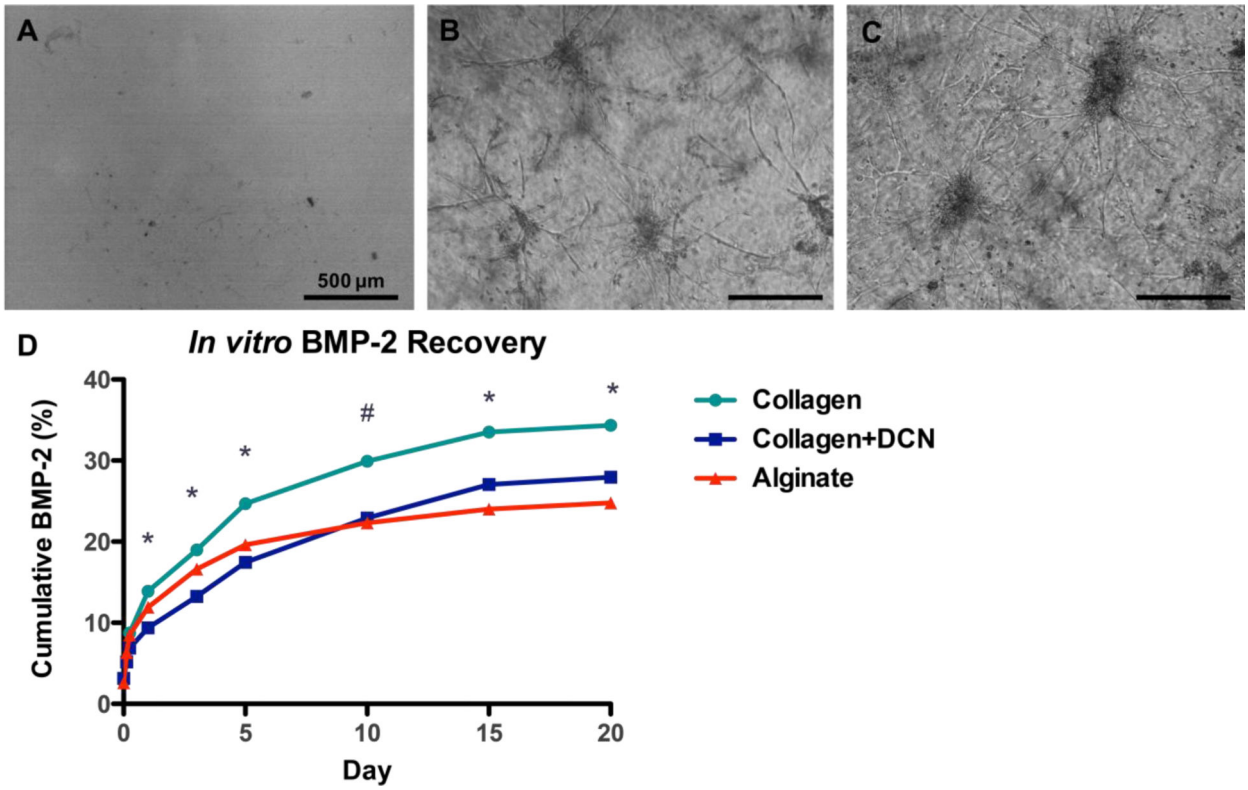

Figure 4.

MVF at day 6 of culture in A) RGD-alginate, B) collagen, C) coll+DCN. Scale bar = 500 μm. **D)** Cumulative in vitro BMP-2 released by acellular gels into surrounding media, n=4/group. * $p<0.05$ between all three materials, # $p<0.05$ between collagen and collagen+DCN and collagen and alginate.

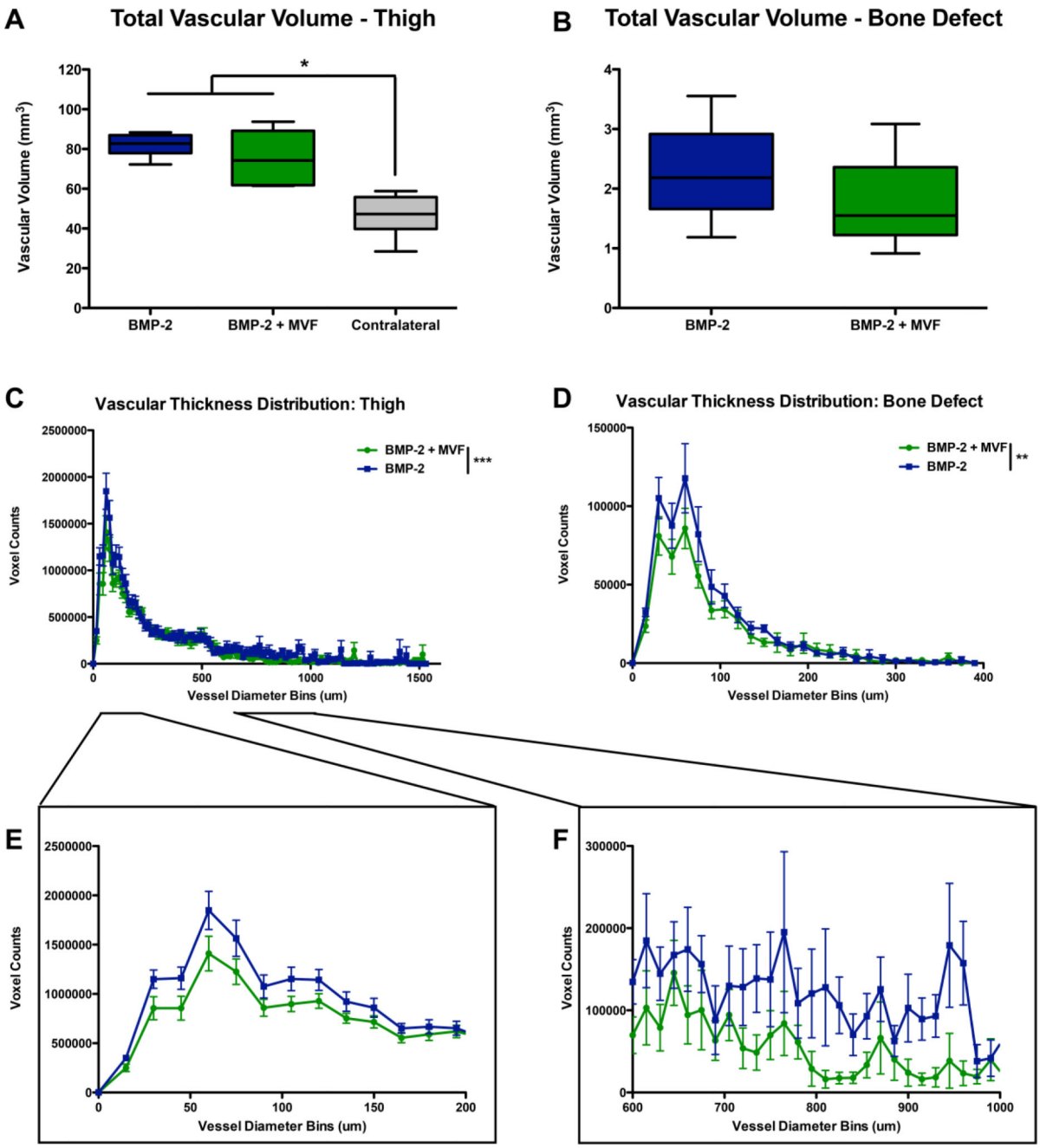

Figure 5.

A) Cumulative in vitro BMP-2 released by acellular vs. MVF-containing collagen+DCN gels into surrounding media, n=5/group. * $p<0.05$, ** $p<0.01$. B) Quantification of total MVF network length and branching without BMP-2 (C) and with 500 ng BMP-2 incorporated into the collagen+DCN gel (D) at day 7 of culture. * $p<0.05$.

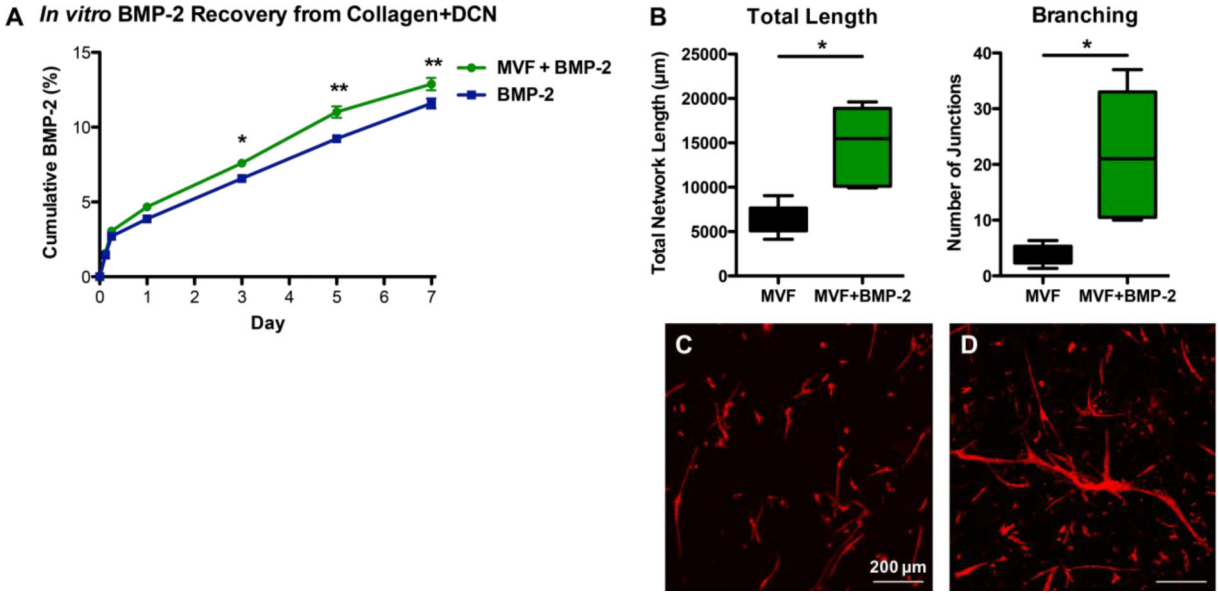

Figure 6.

Quantitative μCT angiography results for total volume of A) the thigh region and B) the bone defect region. n=6/group, * $p<0.0001$ between BMP groups and contralateral control. Vascular thickness distributions for C) the thigh region and D) the bone defect region. Insets show E) small 0–200 μm diameter and F) intermediate 600–1000 μm diameter voxel within the thigh. Voxel counts indicate the number of voxels with a given diameter and are utilized as a measure of vessel number. ** $p<0.01$ between BMP+MVF and BMP (overall effect), *** $p<0.001$.

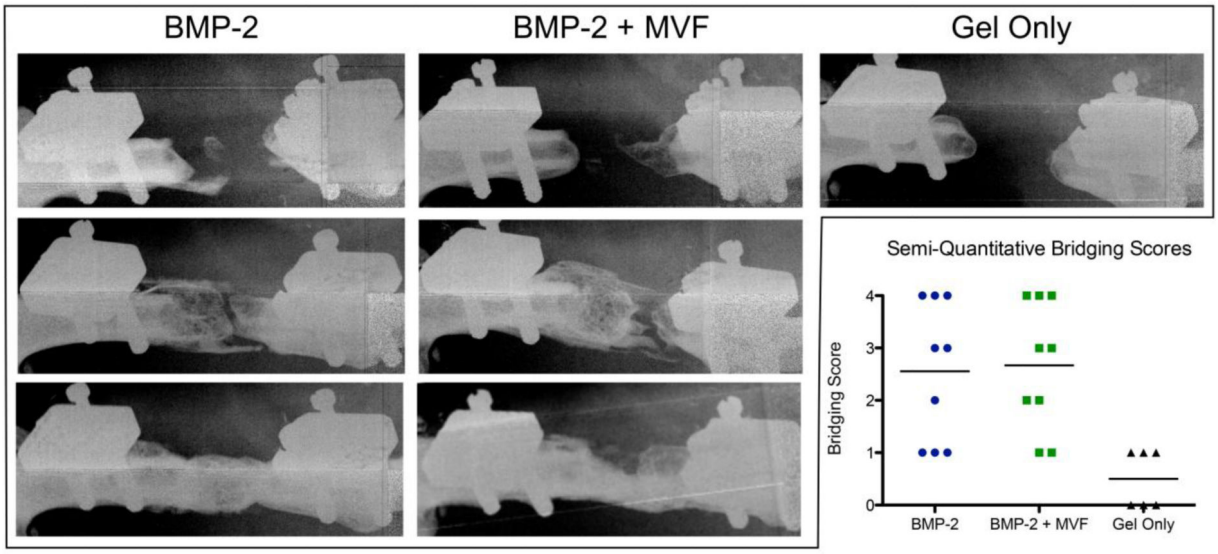

Figure 7.

Representative 12 week radiographs of non-mineralized (top; bridging score 0–1), mineralized but not bridged (middle; bridging score 2–3), and completely bridged (bottom; bridging score 4) samples from each treatment group. The Gel Only group produced only nonmineralized samples. Inset chart shows the semi-quantitative bridging score distribution and mean for each group.

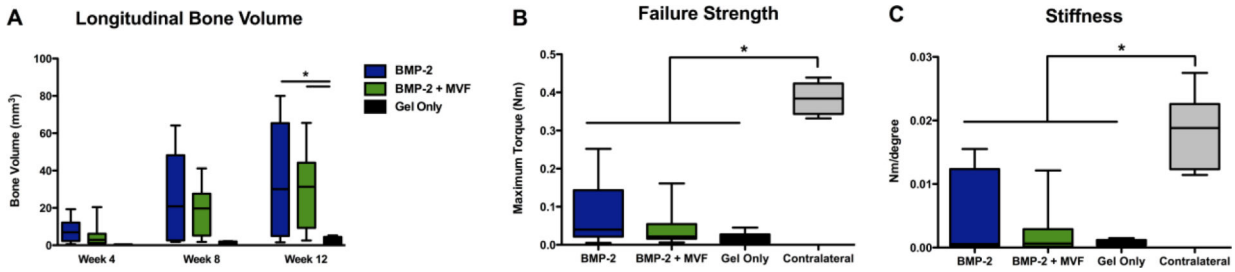

Figure 8.

Longitudinal bone volume as measured with μCT. * p=0.011 between both BMP groups and the Gel Only material control group. B) Failure strength and C) Stiffness of regenerated bone tissue at the 12 week endpoint. * p<0.001 between all treatment groups and the contralateral control.

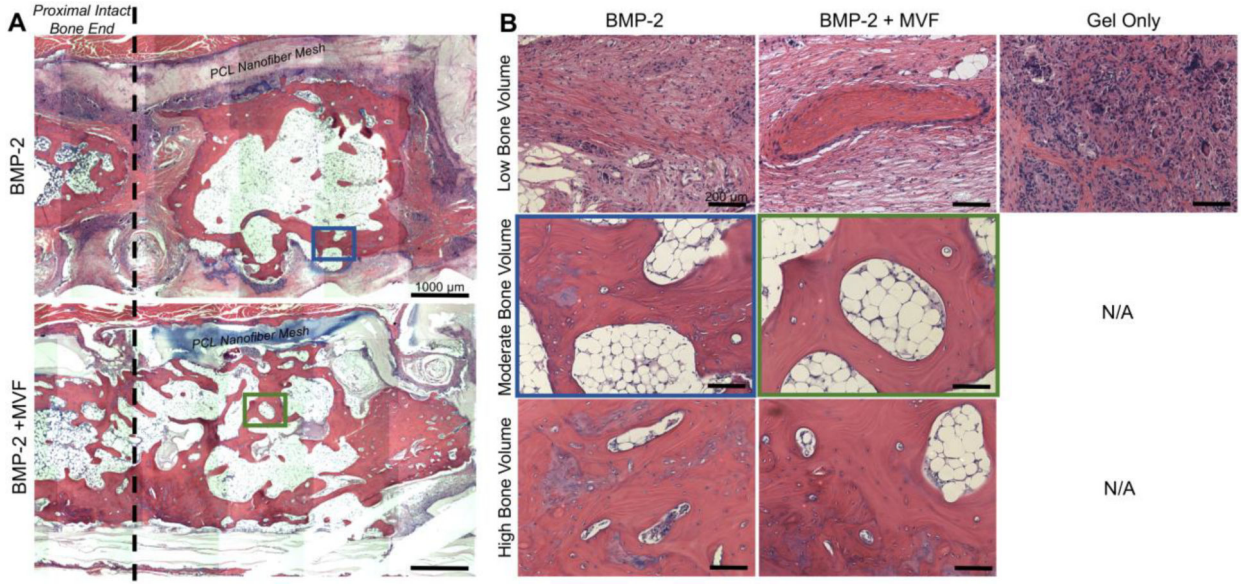

Figure 9.

A) Representative mosaic images of hematoxylin and eosin (H&E) stained samples from the BMP-2 (top) and BMP-2+MVF (bottom) treatment groups. The PCL nanofiber mesh denotes the boundaries of the defect area, and the proximal intact bone end is marked with dotted line. Scale bar = 1000 μm. B) Representative low (top), moderate (middle), and high (bottom) bone volume samples from each treatment group at the 12 week endpoint. The Gel Only group produced only low bone volume samples. Location of moderate bone volume samples within mosaics are outlined in blue and green for the BMP-2 and BMP-2 + MVF groups, respectively. Scale bar = 200 μm.

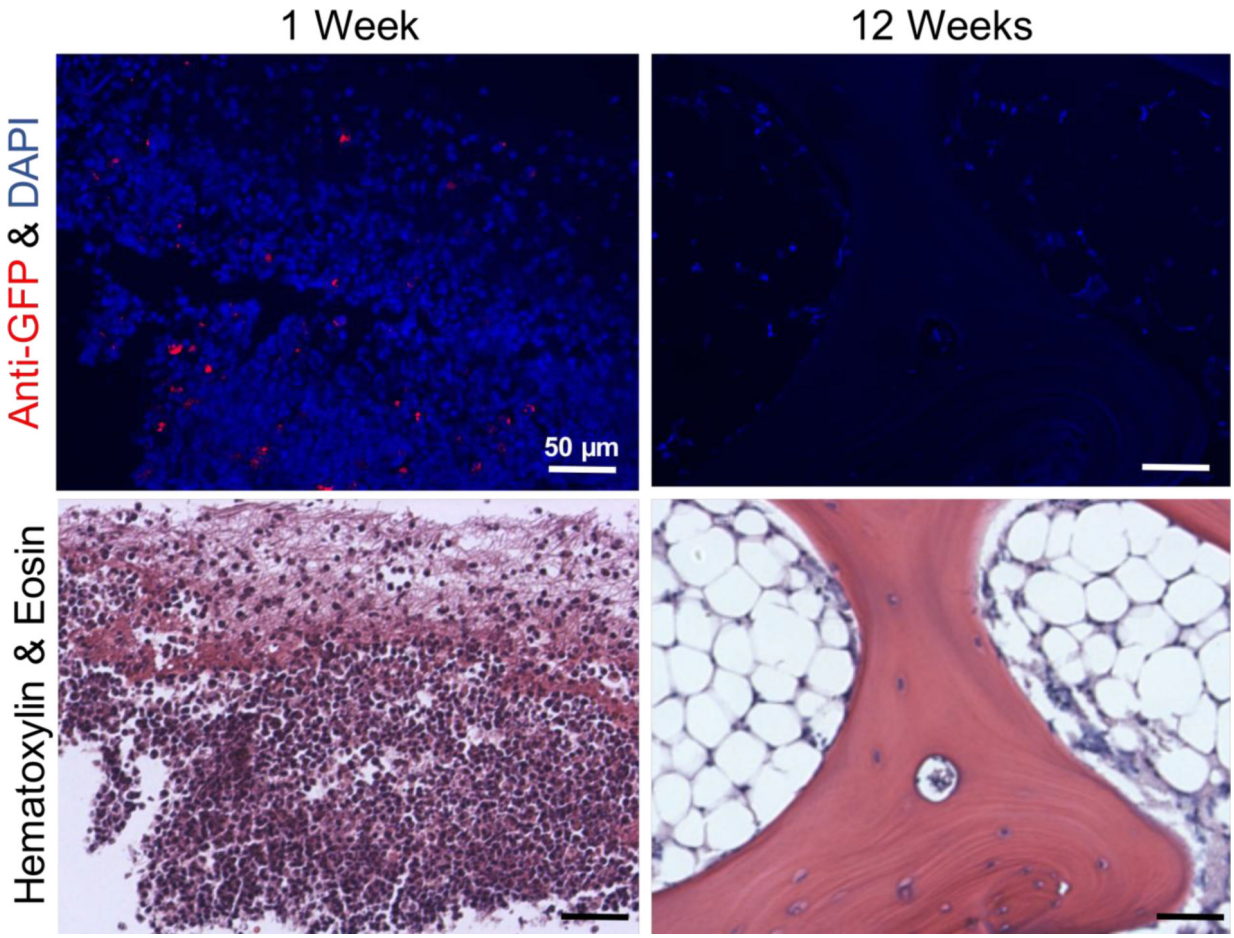

Figure 10.

Anti-GFP immunohistochemistry (top) to identify retention of implanted GFP+ MVF at 1 week and 12 weeks post-surgery. Red - anti-GFP antibody, blue – DAPI. Serial sections stained with H&E (bottom). Scale bar = 50 μm.